



April 2021

Nagercoil Obstetrics and Gynaecological Society

**ULTRASONOGRAPHY FOR FETAL
CARDIAC ANOMALIES**

By

**Dr. Selvapriya Saravanan¹ Dr. Vishakha P. Kandalgaonkar²
Dr. Kunaal K. Shinde^{3*}**



**NAGERCOIL
OBSTETRICS AND GYNAECOLOGICAL SOCIETY
TEAM 2021 - 2022**



Dr. Krishna Surendran
President



Dr. Selvapriya Saravanan
Secretary



Dr. Sudha Sundar
Treasurer

TOGETHER WE CAN, WE WILL.

ULTRASONOGRAPHY FOR FETAL CARDIAC ANOMALIES



Dr. Selvapriya Saravanan¹



Dr. Vishakha P. Kandalgaonkar²



Dr. Kunaal K. Shinde^{3*}

¹Senior Consultant, Dept of Fetal Medicine, Dr. Jeyasekharan Hospital and Director, SPring Fertility – Fetocare - Fetogene, Nagercoil

²Fellow in Fetal Medicine (ICOG), Dr. Jeyasekharan Hospital and SPring Fertility Clinic, Nagercoil

^{3*}Associate Professor and Unit Head, PCMC's Post Graduate Institute, Yashwantrao Chavan Memorial Hospital, Pimpri, Pune

OBJECTIVE:

Fetal cardiac anomalies are common, with half of them being lethal and/or requiring complex surgeries after birth. Early detection of these anomalies enables early referral to tertiary care centers with adequate expertise. A routine antenatal ultrasound performed between 18 and 22 weeks enables detection of most of these malformations. Further comprehensive evaluation can be performed with a dedicated fetal echocardiography, particularly in high-risk pregnancies and in cases with extracardiac anomalies.

This review illustrates the various sonographic techniques for evaluation of fetal heart and the imaging appearance of various fetal cardiac anomalies, and prenatal counselling for the same.

Keywords:

Anomalies, cardiac, fetal, heart, malformations, ultrasound

Congenital cardiac disease is seen in 2–6.5 of 1000 live births and is a major cause of morbidity and mortality, with half of these cases being lethal or requiring surgical correction. Environmental, genetic, and chromosomal abnormalities are believed to be causes of congenital cardiac defects, with a higher incidence among infants with affected siblings or mother. Extracardiac abnormalities are associated with 25% of these cases [1,2].

Detection of cardiac anomalies can be challenging and is typically done by fetal cardiac ultrasound performed between 18 and 22 weeks. Transvaginal scans can detect anomalies even at 12–13 weeks. Detailed fetal echocardiography is performed in high-risk cases, which could be a result of fetal (extracardiac anomalies, increased nuchal translucency, hydrops, or polyhydramnios), maternal (teratogen exposure, metabolic disorders, congenital heart defect, folic acid deficiency, or autoantibodies), or familial (sibling or father with congenital heart defect and Mendelian syndromes) factors. Detection of anomalies alters the obstetric course and outcome, including reassurance, termination, fetal therapy, mode of delivery, and postnatal referral to a tertiary care center with advanced expertise in management of these patients [2].

This article illustrates the imaging techniques and imaging appearance of various fetal cardiac anomalies seen with various sonographic techniques, and prenatal counselling for the same.

Fetal cardiac Ultrasound:

The first step in fetal cardiac ultrasound is to evaluate the orientation of the fetus within the maternal abdomen that is, fetal laterality (presentation and lie). Orientation is assessed from a transverse section of the fetal abdomen. If the fetal head is found below this level and the spine is posterior, then the left side of the fetus should be located on the right side of the maternal abdomen and the stomach should be on this side (Fig. 1A). On the other hand, if the fetal head is found above this level and the spine is posterior, then the right side of the fetus is located on the right side of the maternal abdomen and the stomach is located on the opposite side [3] (Fig. 1B). Situs is the position that an organ occupies in relation to the bilateral body symmetry. For atrial situs, this is the relationship of the atria with respect to each other. This is conventionally established by noting the arrange

mentofthe aorta and inferior vena cava (IVC) at thelevel of the diaphragm, because great vesselarrangementissimilartothoracicandatrial situs. In situs solitus, the IVC is anterior andto the right of the aorta (Fig. 2A). In situs inversus, there is a mirror image pattern, withthe aorta to the right of the IVC (Fig. 2B). In situs ambiguous, the aorta and IVC are located on the same side of the spine in rightisomerism (Fig.2C)andtheaortaiscentrallylocated,withaninterruptedIVCinleftisomerism[3] (Fig.2D).

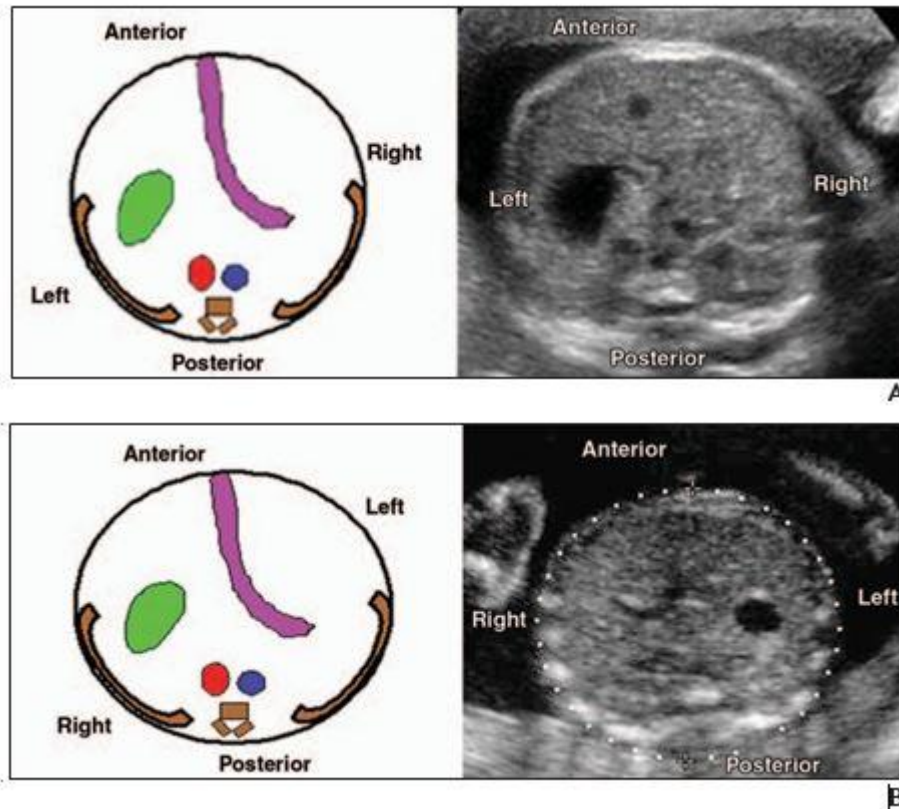


Fig.1—Establishing laterality. Schematic diagram and ultrasound through abdomen show spine and stomach.

A, In this fetus, fetal head was located below plane of abdomen (vertex presentation), making left side lower; hence, stomach was located on left side of fetus.

B, In this fetus, fetal head was located above plane of abdominal image, making left side upper; hence, stomach was located on right side of fetus.

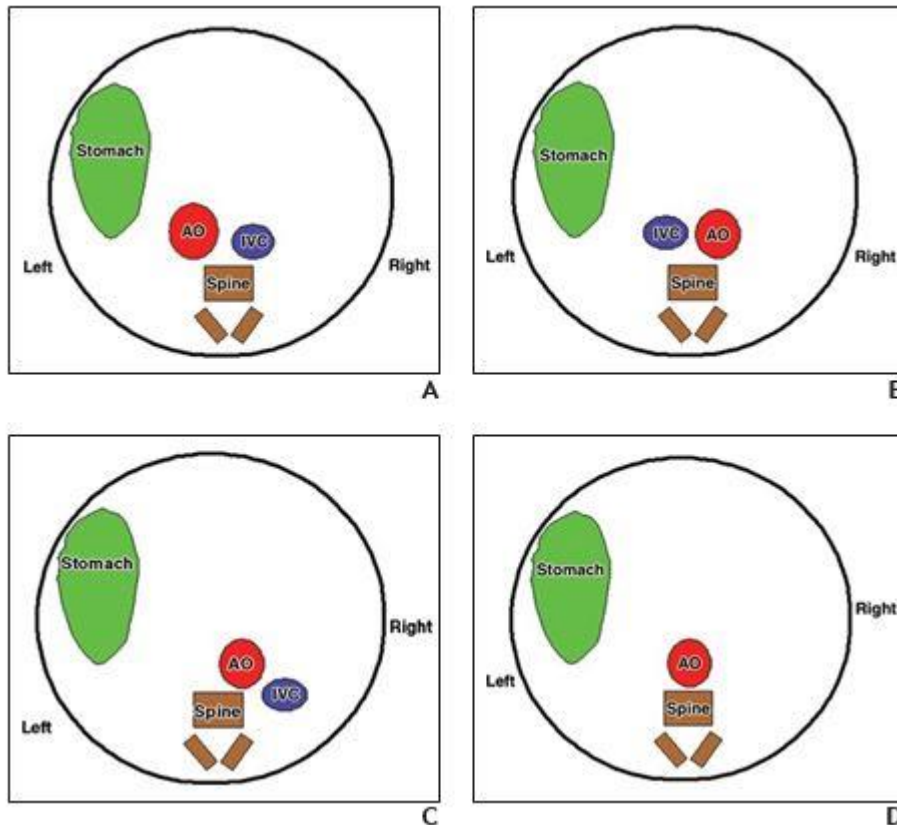


Fig. 2—Establishing situs and atrial arrangement. Diagrams represent axial images acquired at level of lower thoracic spine.

A, In situs solitus, aorta (AO) is located to left of inferior vena cava (IVC).

B, In situs inversus, AO is located to right of IVC.

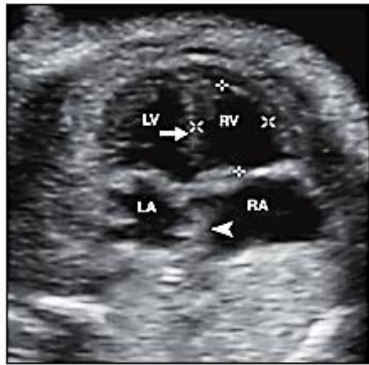
C, In right isomerism, AO and IVC are relocated on same side of spine.

D, In left isomerism, AO is located centrally, and IVC is not visualized because it is interrupted.

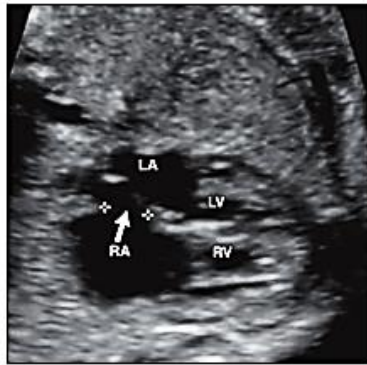
Views in Fetal Cardiac Ultrasound:

The basic view performed in cardiac ultrasound is the four-chamber view [4], which can detect 43–96% of fetal anomalies [1]. “Extended basic views” of the left ventricular outflow tract (LVOT) and right ventricular outflow tract (RVOT) increase the sensitivity for the detection of anomalies. The four-chamber view is obtained by a transverse projection through the fetal thorax above the level of the diaphragm, either apical (parallel to the interventricular septum) or subcostal (perpendicular to the interventricular septum). This view shows the two atria and ventricles along with atrioventricular (AV) valves (mitral and tricuspid) and septa (interventricular and interatrial) (Fig. 3). The cardiac position and axis are determined in this projection. In levocardia, the heart is located within the left chest, with the apex pointing to the left; in dextrocardia, it is located within the right chest with the apex pointing to the right; and in mesocardia, it is centrally located

with the apex pointing anteriorly. The cardiac axis is calculated from a line drawn from the posterior spine to the anterior sternum (spinosternal line). The ventricular septum typically intersects this line at 40–45°. Cardiac axis may be altered in intracardiac conditions (Ebstein's anomaly and tetralogy of Fallot) or extracardiac conditions causing mass effect or as a result of accompanying pulmonary hypoplasia [5].



A



B

Fig. 3—Standard cardiac view.
A, Basic four-chamber view, which shows right ventricle (RV), left ventricle (LV), right atrium (RA), and left atrium (LA). Interventricular septum (arrow) is also seen in this view that is acquired perpendicular to ultrasound beam. Interatrial septum (arrowhead) is visualized.
B, Four-chamber view in another fetus shows patent foramen ovale (arrow).

Cardiac anatomy is typically evaluated using a sequential segmental approach, which depends on morphologic identification of the atria, ventricles, and great arteries, not on their spatial relationship [3]. The morphologic right atrium (RA) has a triangular appendage, whereas the morphologic left atrium (LA) has a hook-shaped appendage. Differences between the morphologic right ventricle (RV) and the left ventricle (LV) are listed in Table 1 [5]. The tricuspid valve opens into the RV and the mitral valve opens into the LV, with the septal leaflet of tricuspid valve inserting more apically than the mitral valve. Occasionally, valves may be imperforate, common, straddling, or overriding. The AV junction is the continuation of atria with the ventricular chamber. In the typical biventricular connection, each atrium connects with a ventricular chamber, which could either be concordant (i.e., RA-RV and LA-LV), discordant (i.e., RA-LV and LA-RV), or ambiguous (i.e., isomeric RA or LA with RV to the right or left of LV). In univentricular connection, one or two atrial chambers connect with a single ventricular cavity [3]. There are two arterial valves, the aortic and pulmonary, which connect the LV to the aorta and the RV to the pulmonary artery (PA), respectively. Ventriculoarterial connections can be concordant (i.e., aorta from LV and PA from RV), discordant (i.e., aorta from RV and PA from LV), double outlet (i.e., >50% of each great artery connected to same ventricular cavity), and single outlet (i.e., only one arterial trunk connected to the ventricle). The LVOT view is obtained by a 45° tilt of the transducer from the four-chamber view perpendicular to the septum, to an oblique plane from the fetal upper left quadrant of the abdomen to the fetal right shoulder. The aorta originates from the LVOT (Fig. 4A) and dis-

tally gives off the great vessels of the head and neck. Membranous septum is also visualized in this view. The RVOT view can be obtained by further rotation in the same direction and gentle rocking of the transducer from the LVOT view. The PA is seen exiting from the RV (Fig. 4B), dividing into the right PA and left PA (Fig. 4C) and continuing as the ductus arteriosus, which opens into the descending thoracic aorta (Fig. 5). The ascending aorta is seen centrally, wrapped by the RV and PA. In both of these projections, a normal aorta and PA are perpendicular to each other. Further rightward rotation results in short-axis views of the ventricles and thorax. Further rotation toward the left fetal shoulder shows the aorta as a central circle draped by the PA anteriorly and to the left. Rotation from the left shoulder to the right hemithorax shows the aortic arch and its branches (Fig. 5A) and ductus arteriosus (Fig. 5B). The ductal arch (RVOT, PA, and ductus arteriosus) is broader and flatter than the aortic arch.

A comprehensive set of five short-axis projections can also be acquired, with the ventricular septum parallel to the ultrasound beam. These views are better at detection of conotruncal abnormalities that are missed by the routine views. From caudad to cephalad, these views are the abdomen at the level of the stomach to identify situs; the four-chamber view; the five-chamber view, which includes a centrally placed aorta; PA bifurcation, with the PA originating from the RV located on the left side and crossing the aorta to lie to the left side and anterior of aorta; and the three-vessel view, which includes the main PA, ascending aorta, and superior vena cava (SVC) from the left anterior to the right posterior aspect of the thorax [5] (Fig. 6). The SVC typically opens into the RA (Fig. 5C). Pulmonary veins typically drain into the LA, but anomalous veins can drain into systemic veins, either partially or totally [3] (Fig. 5D)

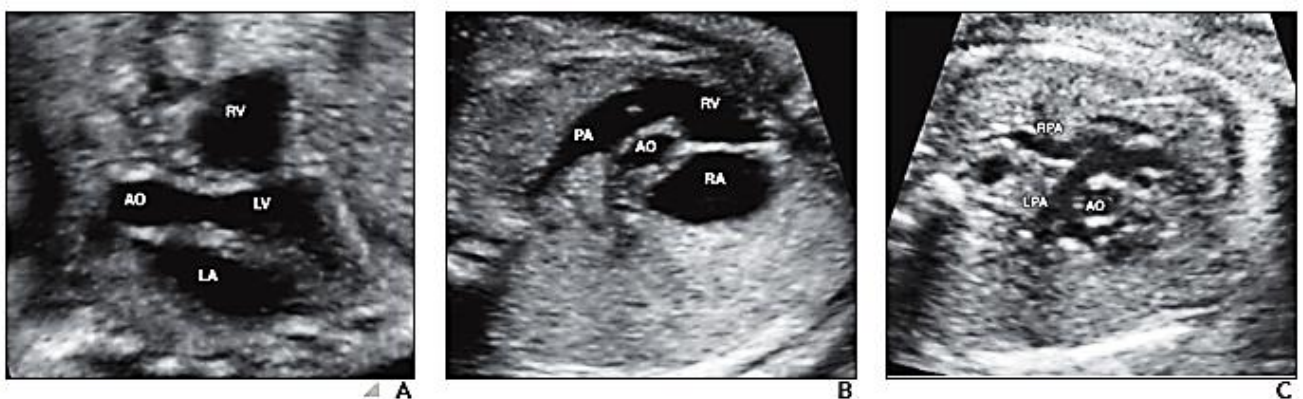
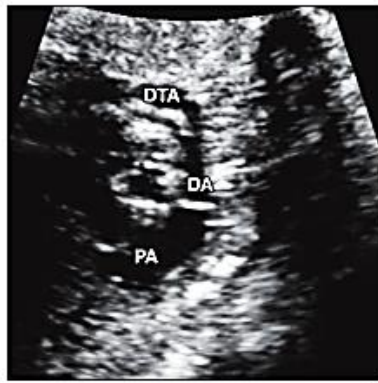


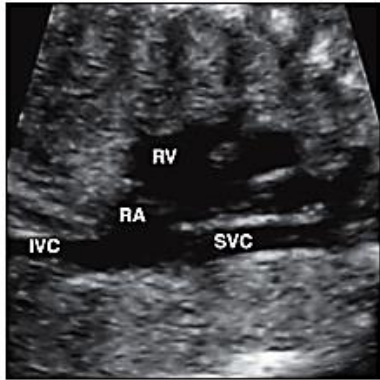
Fig. 4—Extended cardiac views.
 A. left ventricular outflow tract view shows left ventricle (LV), which gives origin to ascending aorta (AO). Right ventricular (RV) outflow tract and left atrium (LA) are also seen.
 B. Right ventricular outflow tract view shows RV, giving origin to main pulmonary artery (PA). AO is seen as circular structure and is perpendicular to PA.
 C. Further superiorly, right pulmonary artery (RPA) and left pulmonary artery (LPA) are seen.



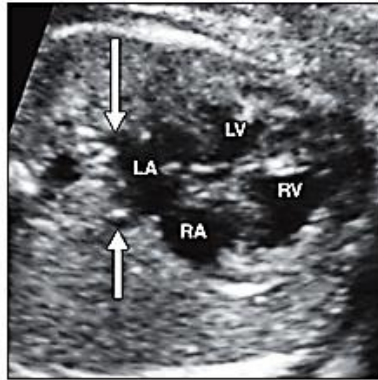
A



B



C



D

Fig. 5—Vascular structures.
 A, Aortic arch can be seen giving off branches to head and neck and continuing as descending thoracic aorta (DTA). DA = ductus arteriosus.
 B, DA connects pulmonary artery (PA) to DTA.
 C, Superior vena cava (SVC) and inferior vena cava (IVC) open into morphologic right atrium (RA). RV = right ventricle.
 D, Pulmonary veins (arrows) open into morphologic left atrium (LA). LV = left ventricle.

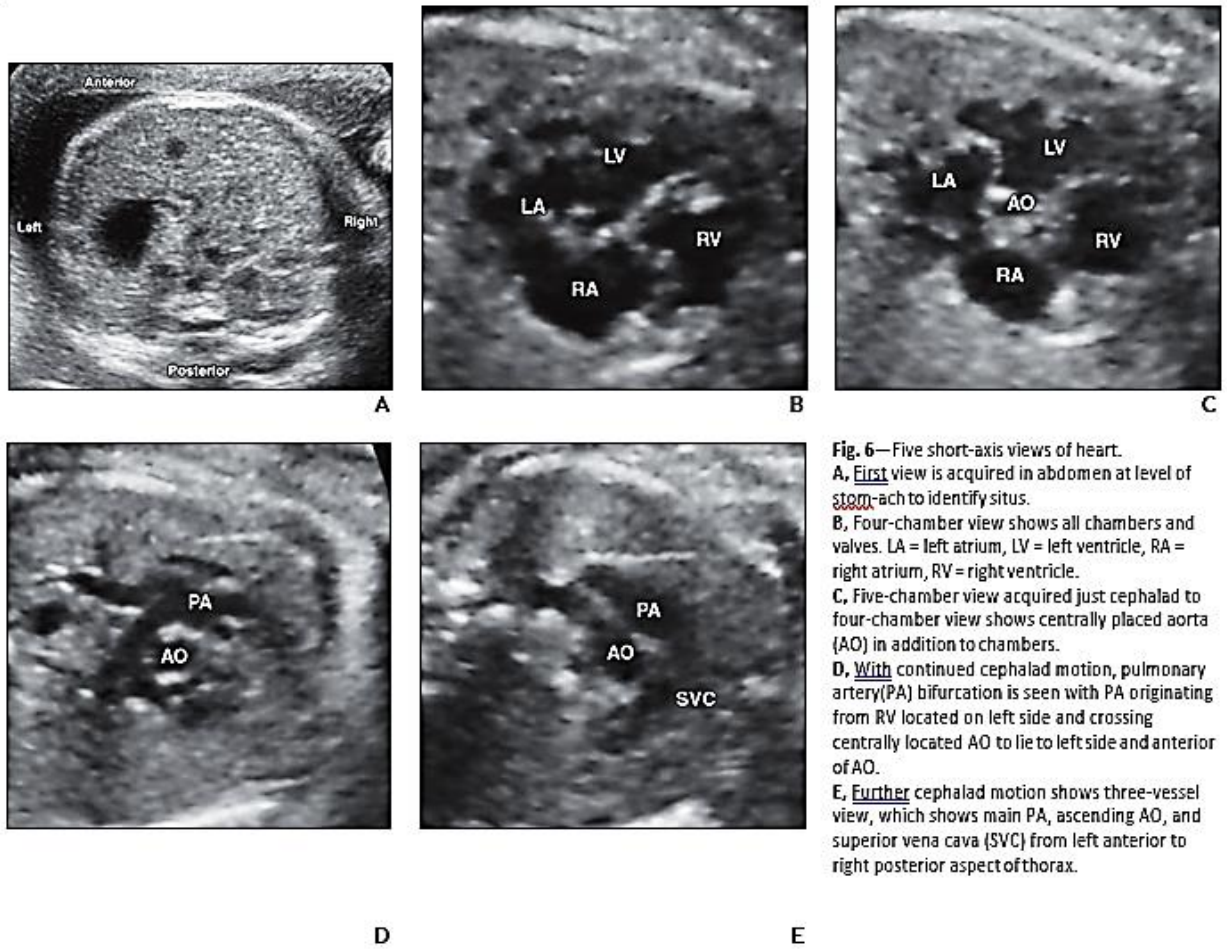


Fig. 6—Five short-axis views of heart.
A, First view is acquired in abdomen at level of stomach-ach to identify situs.
B, Four-chamber view shows all chambers and valves. LA = left atrium, LV = left ventricle, RA = right atrium, RV = right ventricle.
C, Five-chamber view acquired just cephalad to four-chamber view shows centrally placed aorta (AO) in addition to chambers.
D, With continued cephalad motion, pulmonary artery (PA) bifurcation is seen with PA originating from RV located on left side and crossing centrally located AO to lie to left side and anterior of AO.
E, Further cephalad motion shows three-vessel view, which shows main PA, ascending AO, and superior vena cava (SVC) from left anterior to right posterior aspect of thorax.

Measurements:

The cardiac chambers and vascular structures are measured and can be compared with normalized charts. The RV and LV typically are of the same size, with a 1:1 ratio. The cardio thoracic ratio is the ratio between the cardiac and thoracic circumferences, which normally measures 0.5 [6]. Normalized charts at various gestational age exist for the RV: LV ratio, LV wall thickness, septal wall thickness, left atrial dimension, PA diameter, and aortic root diameter. A small heart is seen as a result of hypoplasia (LV or RV or both) or of compression from extrinsic masses, whereas a large heart can be seen in various congenital abnormalities, pericardial effusion, aneurysms, cardio myopathies, and tumors. The PA diameter is typically larger than the aorta by approximately 10%. However, as a general rule, the two can be considered to be similar in size and any discrepancy in size should be concerning.

M-mode Ultrasound:

M-mode ultrasound is a 2D image of motion over time that is used for evaluation of fetal heart motion, heart rate, wall thickness, chamber size, and motion of the valves or myocardium. Fetal heart rate and rhythm can be evaluated using M-mode ultrasound through the atrial and ventricular wall, above and below the AV valve, respectively. Chamber size and function are evaluated by focusing at the level of AV valves [6]. AV concordance can be evaluated by using M-mode ultrasound through both atrium and ventricle at the same time. Normal fetal heartbeats are 175 beats/min at 8 weeks, 140 beats/min at 20 weeks, and 130 beats/min at term [5], with a regular 1:1 AV rhythm [5].

Colour-Flow Pulsed Doppler and Doppler Tissue Imaging:

Color Doppler can be used to detect vascular flow through cardiac chambers, vascular structures, and septal defects. It also significantly reduces the time required for Doppler examination of the heart, because interrogation of vascular structures becomes easier [1]. The direction of the flow can be established, which is useful in the detection and quantification of regurgitation and stenosis. Reversal of the flow through a valve indicates regurgitation. The presence of aliasing in color Doppler indicates high velocities suggestive of stenosis. If pulsed Doppler is applied at this point, high velocity with spectral broadening can be seen. Normal peak velocity through the AV valves is 30–60 cm/s throughout gestation, and that through the arterial valves is 25 cm/s at 12 weeks and 60–100 cm/s by term [6]. Color Doppler is also used in the evaluation of pulmonary and systemic venous connections and small septal defects. Color Doppler tissue imaging has been used recently for evaluating high-amplitude low-velocity signals, such as within the moving myocardium. This can be used to encode the direction of myocardial motion, which is particularly useful in the assessment of arrhythmias [7].

Three and Four-Dimensional Ultrasound:

In 3D ultrasound, volumetric data are acquired from a single window using few seconds of scanning, which are subsequently used for reconstruction of multiple views in any plane. This reduces the overall scanning time and the

operator and window dependence, in addition to improving the assessment of cardiac anatomy. Planes that are not accessible in 2D scanning, such as the interventricular septum or coronal plane, can be reconstructed. Volume-rendered or surface-shaded images give an illusion of depth, which might be useful in the detection of complex anomalies, such as those involving the conotruncal septum. Alternatively, the images can be displayed as three or four simultaneous multiplanar reformatted projections with the ability to move through the volumes. Three-dimensional quantitative measurements are more accurate and reproducible than 2D techniques. Acquisition of temporal information with cardiac gating enables display of these images as cine loops in multiple planes (4D imaging), which is useful in the evaluation of cardiac motion, cardiac function, valvular function, volumes, and cardiac output. Three-dimensional imaging of regurgitation and stenotic jets is possible when 3D ultrasound is combined with color or power Doppler imaging. Three-dimensional color-flow angiography can reveal complex cardiovascular anatomy, anomalous vessels, and small septal defects [7].

Atrial Septal Defect:

Atrial septal defect (ASD) is characterized by a defect in a portion of the atrial septum. It is the fifth most common congenital heart disease, seen in 1 of 1500 live births [1], and is caused by abnormal tissue resorption and deposition during development of the atrial septum. According to its location, it is classified as ostium secundum (midatrial septum), ostium primum (lower atrial septum) (Fig. 7), sinus venosus (outside the atrial septum in the wall separating the SVC or IVC from the LA), and coronary sinus defect, which can be partial or complete. ASD may be difficult to visualize in a fetus because of the presence of foramen ovale. However, with high-resolution ultrasound, the septum primum is seen in the four-chamber view as a circular or linear structure with a loose pocket configuration, and the septum secundum is seen as a thick stationary structure with the foramen ovale opening into it. Normal foramen ovale measures almost the same as the aortic root, with the difference being 1 mm or less [1] (Fig. 3B). The foramen flap of the foramen ovale is seen moving into the LA at twice the heart rate. A secundum defect is seen as a larger defect in the central portion of the atrial septum or a deficient foramen flap. A primum defect is seen in the lower part of the atrial septum.

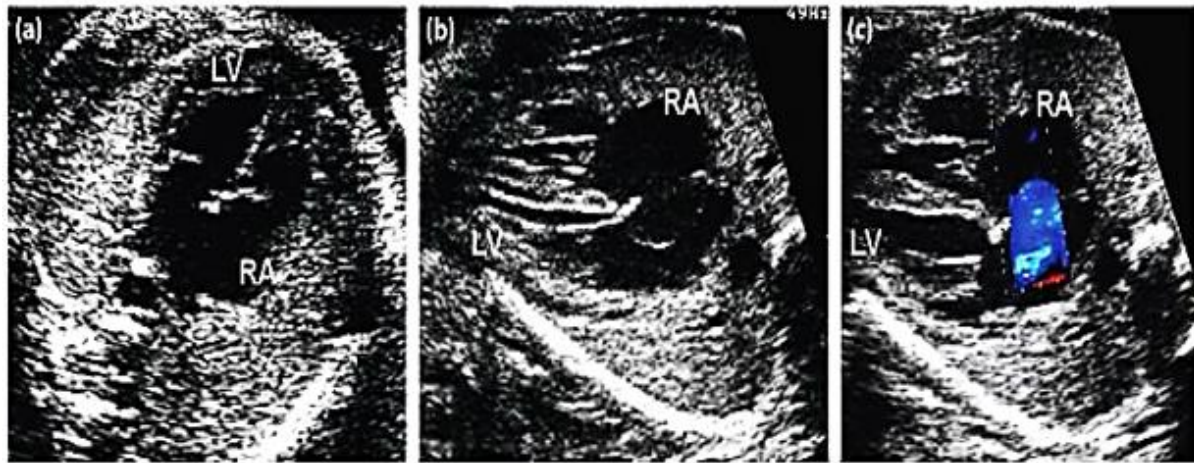


Fig. 7. Atrial Septal Defect: two cases of ASD confirmed at birth.

- a. On the apical four-chamber view, an extremely wide (8 mm) foramen ovale can be seen.
- b. Also, in this case, on the transverse four chamber view, the large size of the foramen ovale is evident; the flap is seen in the left atrium.
- c. Same case as in (b): colour Doppler demonstrates the extent of the shunt.

LV: left ventricle RA: right atrium

Counseling:

If ASD is isolated, as in most instances, survival and quality of life are unaffected, regardless of the need for an interventional procedure. Only in the unlikely case in which an ASD is detected late, when it has already caused irreversible pulmonary hypertension, does the life expectancy decrease and there may be severe complications adversely affecting survival and quality of life.

Ventricular Septal defect:

Ventricular septal defect (VSD) is the most common congenital heart disease, seen in 1.5–3.5 per 1000 live births, and accounting for 30% of all cardiac anomalies [8]. The defect is most commonly (80%) seen in the membranous septum and less commonly in the

muscular, outlet, or inlet portions. Defects can be variable in size. VSD is best seen in a four-

chamber view as discontinuity in the ventricular septum, particularly the inlet defects. The ventricular septum is ideally evaluated in images acquired perpendicular to the interventricular septum because a pseudo-VSD, as a result of signal drop-out, can be seen in the superior aspect of images parallel to the ultrasound beam [8]. Membranous septum is also seen in the LVOT view. Out-let defects are best seen when the transducer is angled anteriorly [3]. Small defects can be difficult to detect, particularly in the perimembranous portion, but Doppler imaging can show flow across the defect. In isolated VSD, bidirectional shunting with right-to-

leftshuntduringsystoleandleft-to-rightshuntingindiastoleisseen,butinVSDassociatedwithotheranomalies,unidirectionalshuntingmaybeseen.Smalldefectsmayclose,butlargedefectsrequiresurgicalclosure.

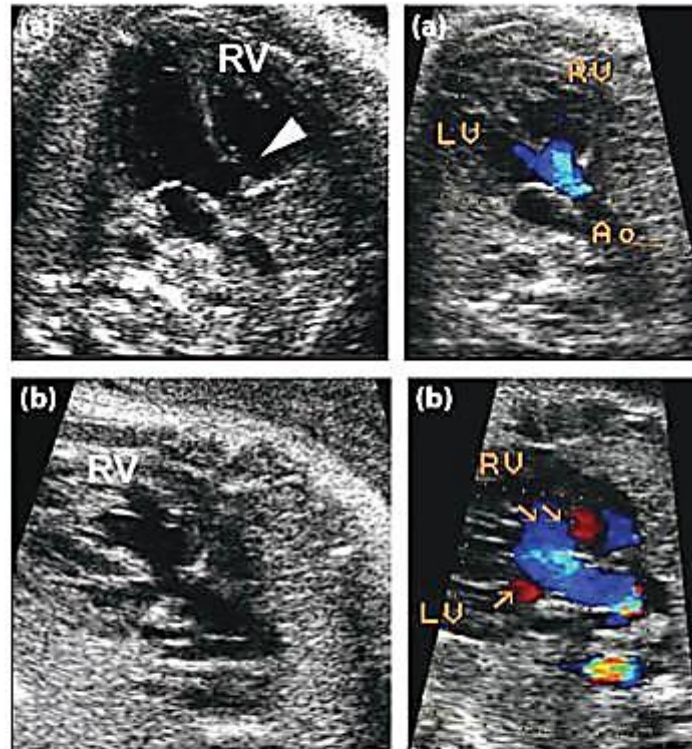


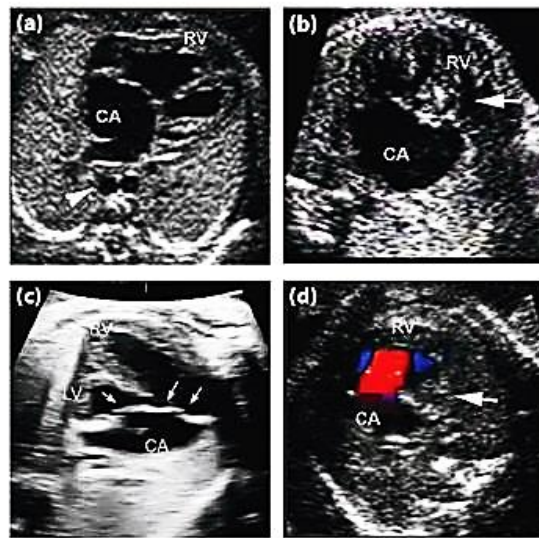
Figure 1 Ventricular septal defect (VSD). VSDs not detectable on the four-chamber view but only on the left outflow tract view which include (a) outlet subaortic perimembranous VSD (color Doppler demonstration on the right, 31 weeks of gestation); and (b) malalignment VSD, with the ascending aorta overriding the VSD (color Doppler demonstration on the right, 27 weeks of gestation). Ao: aorta; LV: left ventricle; RV: right ventricle.

Counseling:

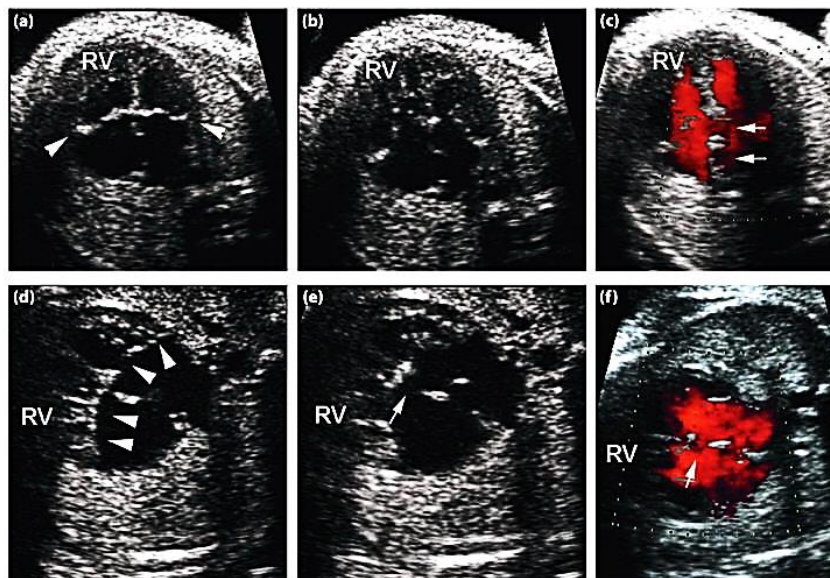
In postnatal series, the prognosis for isolated VSDs is extremely favourable, with a high rate of spontaneous closure (upto 90% of cases, if the smallest muscular defects are included) and normal life expectancy both for untreated nonrestrictive VSDs and for large ones, if operated. In contrast, prenatal series show lower survival rates, as is often the case when comparing prenatal and postnatal data for CHD: the intrauterine mortality rate can reach 11% and the neonatal mortality rate 31%, with a five year survival rate of 40%.

AV Septal Defect:

AV septal defect (AV canal defect or endocardial cushion defect) is caused by failure of fusion of the endocardial cushion, resulting in defects of the atrial ostium primum, the ventricular inlet septum common AV valve, and the biventricular AV connections. AV septal defect accounts for 2–7% of congenital heart defects and is seen in 0.19–0.56 per 1000 live births [8]. It is associated with trisomy 21 syndrome, left atrial isomerism, hypoplastic left heart, pulmonary stenosis, coarctation, tetralogy, complete heart block, and extracardiac anomalies. There are two types: the complete type (97% of cases), with common valvular orifice, and the incomplete type, with separate right and left valve orifices. The valve of common AV junction has five leaflets, which are separate in the complete type, but two leaflets are connected by narrow tissue in the incomplete type. It is associated with a cleft in the anterior mitral leaflet. Free regurgitation is seen across the common AV valve [8]. Direct shunting may be seen from the LV into the RA. In severe forms, all four chambers communicate, causing left-to-right and right-to-left shunt. Ultrasound shows a defect in the endocardial cushion, with an inlet VSD and primum ASD (Fig.) associated with a single abnormal AV valve that has a T-shaped arrangement. Color Doppler shows open flow across the defect and abnormal AV valve.



Atrioventricular septal defect (AVSD) complete, unbalanced in atrial isomerism (21–22 weeks of gestation). (a) Moderate ventricular disproportion (right ventricle larger than left). However, the azygos continuation (arrowhead) adjacent to the descending thoracic aorta should arouse suspicion of a situs abnormality. (b) Unbalanced AVSD, with severe hypoplasia of the right ventricle (arrow). (c) Unbalanced AVSD, with severe hypoplasia of the left ventricle (arrow). (d) In the same case as in (c), color Doppler demonstrates overriding of the atrioventricular valve and obstruction of the left part of the valve, responsible for the hypoplasia. CA: common atrium; RV: right ventricle.

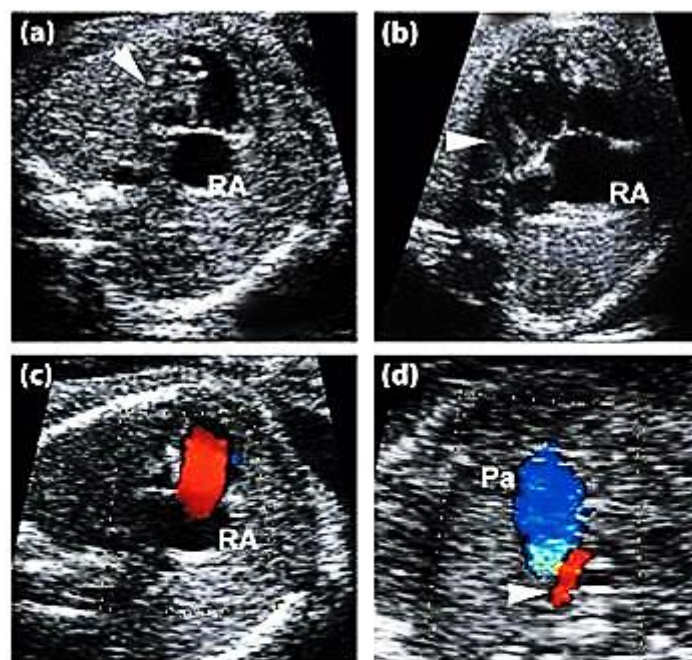


Atrioventricular septal defect (AVSD) partial (29 weeks of gestation). This is characterized by an atrial septal defect (ASD) of the ostium primum type (absence of the septum primum) with two atrioventricular valves, which do not show the normal offset aspect. (a,b) On 2D ultrasound, during systole (a), on the apical four-chamber view, the lack of the normal offset aspect is seen (arrowheads). In diastole (b), two separate atrioventricular valves are demonstrated. (c) Color Doppler helps to confirm the presence of the septum primum defect and, when present, of the VSD (arrows). (d) In systole, but on the transverse four-chamber view, the loss of the offset appearance of the atrioventricular valves is confirmed (arrowheads). (e) In diastole, the ostium primum defect is shown, just above the atrioventricular plane (arrow). (f) Color Doppler demonstrates flow across the ostium primum defect (arrow), across the normal foramen ovale (to the right of the ostium primum), and across the small VSD (to the left of the ostium primum). RV: right ventricle.

Hypoplastic Left Heart Syndrome:

Hypoplastic left heart syndrome is characterized by hypoplastic left-sided cardiac structures, including the LV, mitral valve, aortic valve, and aorta. It accounts for 2–4% of congenital cardiac defects and is seen in 0.16–0.25 per

1000 live births [8]. It is more common in boys and is caused by decreased flow in and out of the LV during development (e.g., mitral or aortic stenosis or atresia). Blood flow to the systemic circulation (coronary arteries, brain, liver, and kidneys) in these patients is dependent on flow through the ductus arteriosus. It is associated with aortic coarctation in 80% of cases [10]. On ultrasound, the LV is small (LV:RV ratio < 1) in size (Fig.); the ventricular septum makes an angle of 90° with the spinosternal line, and the aortic outflow is smaller than the pulmonary outflow tract. Mitral and aortic valves are hypoplastic or atretic. A single area of flow is seen at the AV level and bidirectional flow at the proximal aorta because of distal aortic coarctation [1].



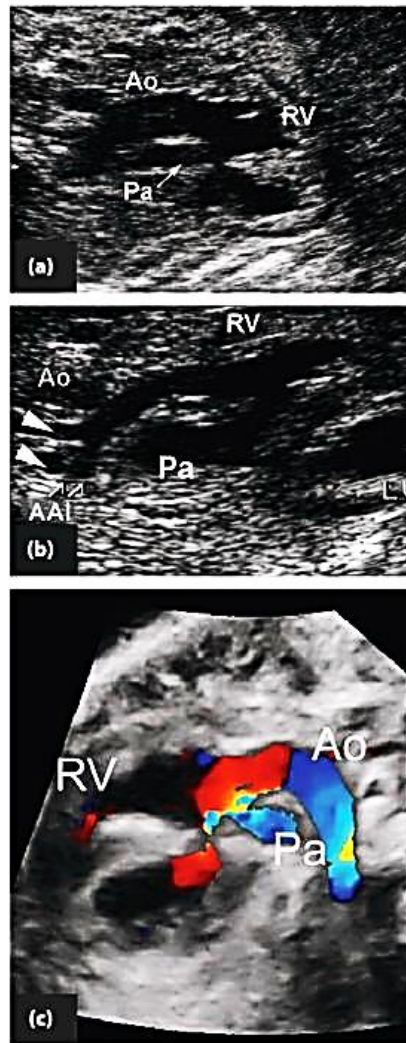
Hypoplastic left heart syndrome. (a) At 22 weeks of gestation, on the four-chamber view, the severe hypoplasia of the left ventricle, transformed into a virtual cavity due to the mitral atresia (arrowhead), is evident. (b) At 32 weeks of gestation, there is severe hypoplasia of the left ventricle, which is slitlike (arrowhead). (c) In the same case as in (a), color Doppler demonstrates the mitral atresia (absence of left ventricular filling). (d) On the three-vessel view, the reverse flow across the hypoplastic aortic arch (in red, arrowhead) (associated tubular hypoplasia) confirms the aortic atresia.

Counseling:

Despite the recent brilliant achievements of paediatric cardio surgery, HLHS continues to be congenital cardiac defect with highest mortality.

Double Outlet Right Ventricle:

Double outlet RV (DORV) is characterized by the origin of more than 50% of both the aorta and PA from the RV and is caused by abnormal spiraling of the truncus arteriosus and the arrest of membranous septal formation. It accounts for less than 1% of congenital heart defects and is seen in 0.08–0.16 per 1000 live births [8]. There are four types of DORV: aorta parallel to the PA and to its right (64%), which resembles tetralogy of Fallot; aorta anterior and to the right of the PA (26%), resembling D-transposition of great arteries; aorta anterior and to the left of the aorta (7%), resembling L-transposition of great arteries; and aorta posterior and to the right of the PA (3%). DORV is almost always associated with VSD, which provides the only outlet from the LV. It is associated with maternal diabetes or alcohol intake and other cardiac defects, such as LV hypoplasia, mitral valve stenosis or atresia, aortic valve stenosis, aortic coarctation or interruption, and coronary artery anomalies. DORV is best seen in short-axis views, where the aorta and pulmonary arteries do not cross and both the vessels arise from the RV and are parallel to each other (Fig.). Demonstration of the origin of both the vessels from the same side of ventricular septum is essential to differentiate DORV from transposition of great arteries [8].



Double-outlet right ventricle (DORV). This comprises a spectrum of anomalies of the great vessels, which may have different sizes due to left or right outflow obstruction, in different spatial relationships (see text of this chapter). (a) DORV with an anterior malposed aorta and a posterior moderately stenotic pulmonary artery (arrow); this is one of the most common arrangements seen in the fetus. (b) DORV with an anterior malposed aorta, which is also reduced in size due to a concurrent interruption of the aortic arch; note the straighter course of the aorta and the “V” shape of the first neck vessels (arrowheads). (c) Color Doppler can be used to confirm the connection of the great vessels with the anterior ventricle, if there is any remaining doubt regarding the differential diagnosis with transposition of the great arteries. AAI: aortic arch interruption; Ao: ascending aorta; Pa: main pulmonary artery; RV: right ventricle.

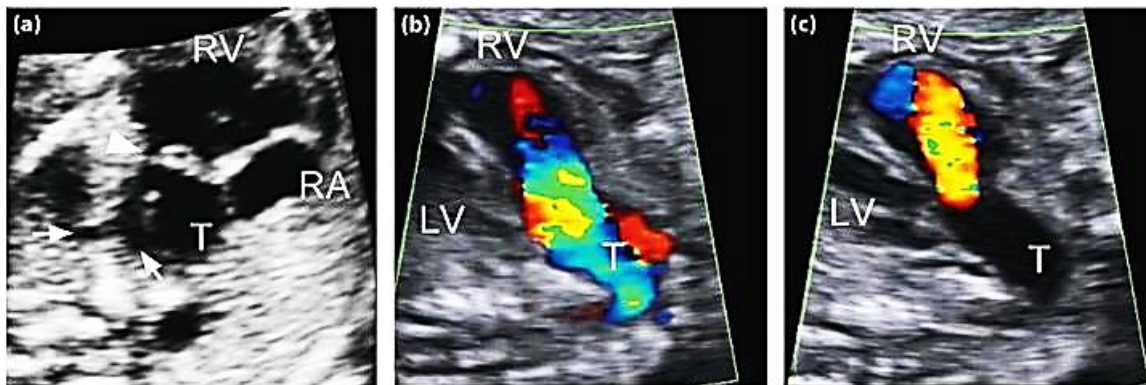
Counseling:

The overall survival of DORV detected prenatally is 46-50% (if terminations of pregnancy are excluded), due to the strong association with aneuploidy and extra cardiac anomalies.

Truncus Arteriosus:

Truncus arteriosus is characterized by a single arterial trunk that feeds

the systemic pulmonary circulation and coronary arteries with a single semilunar valve. It accounts for 1–2% of congenital cardiac defects, is seen in 0.08–0.16 per 1000 live births [8], and is caused by failure of fusion and descent of the conotruncal ridge. It almost always straddles a VSD and receives blood from both the ventricles but rarely originates almost completely from the RV or LV. There are four types (Collett-Edwards classification) based on the level of origin of the aorta and pulmonary arteries [9]. An admixture of oxygenated and deoxygenated blood in the common trunk results in subnormal systemic oxygenation. The ductus arteriosus is not necessary for systemic flow and therefore does not fully develop. On ultrasound, a single arterial trunk is seen overriding the interventricular septum, with an associated VSD, and there are several branches connecting with the aorta and pulmonary vasculature (Fig.)



Common arterial trunk (CAT), type I, 23 weeks of gestation. (a) The main pulmonary artery with the two hypoplastic branches (arrowheads) is seen branching off the truncus (T) just above the truncal valve (arrowhead). (b) On the left outflow tract view, color Doppler demonstrates (during systole) moderate stenosis of the truncal valve (aliasing and turbulence), due to a highly dysplastic truncal valve. Straddling of the truncus toward the right ventricle is also visible. (c) During diastole, massive insufficiency of the dysplastic truncal valve is visible. Note how the truncus is prevalently connected to the right ventricle due to the straddling. LV: left ventricle; RV: right ventricle; T: arterial trunk.

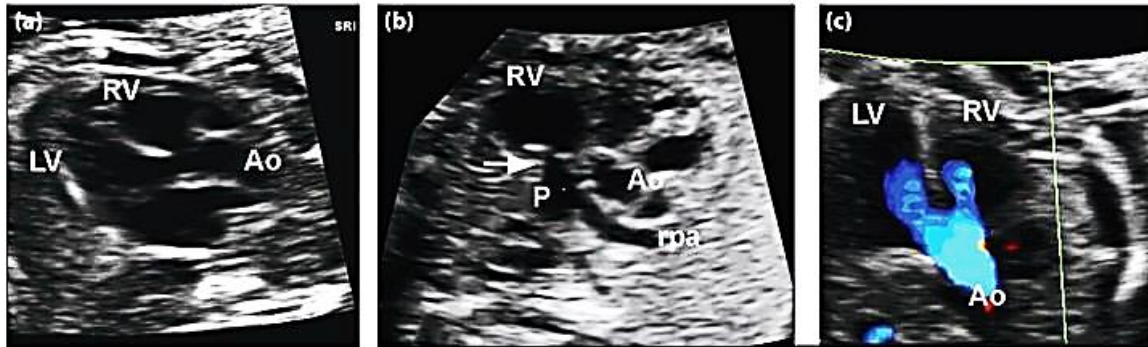
Counseling:

Prognosis depends on the presence of extracardiac and chromosomal anomalies and of unfavourable cardiac anatomy. (e.g. severe truncal valve regurgitation, IAA, and straddling with ventricular hypoplasia)

Tetralogy of Fallot:

Tetralogy of Fallot is characterized by narrowing of the RVOT, VSD, overriding aorta, and right ventricular hypertrophy. It accounts for 5–10% of congenital cardiac defects and is seen in 0.24–0.56 per 1000 live births [8]. It is caused by anterior displacement of the conotruncus, resulting in unequal division of conus into a small anterior RV portion and large posterior LV portion. The incomplete closure of this septum results in aortic overriding. It is associated with chromosomal and extra-

cardiac abnormalities. On ultrasound, the aorta is seen straddling a large membranous VSD (Fig. 9). Depending on the size of the PA, it may not be easily seen and the normal crossing of aorta and pulmonary arteries is not seen. The aorta may be dilated, and the pulmonary valve is stenosed or atretic with a dilated PA. Because of the presence of normal fetal shunts, RV hypertrophy is not seen in the fetus.



Tetralogy of Fallot (TOF): the typical signs of TOF are shown. (a) The left outflow tract view shows a malalignment VSD with an overriding aorta. (b) The right outflow tract view shows the narrowing of the pulmonary trunk, consistent with an infundibular stenosis (arrow). (c) On the left outflow tract, color Doppler demonstrates the overriding aorta draining from both ventricles. Ao: aorta; LV: left ventricle; P: pulmonary artery; rpa: right pulmonary artery; RV: right ventricle.

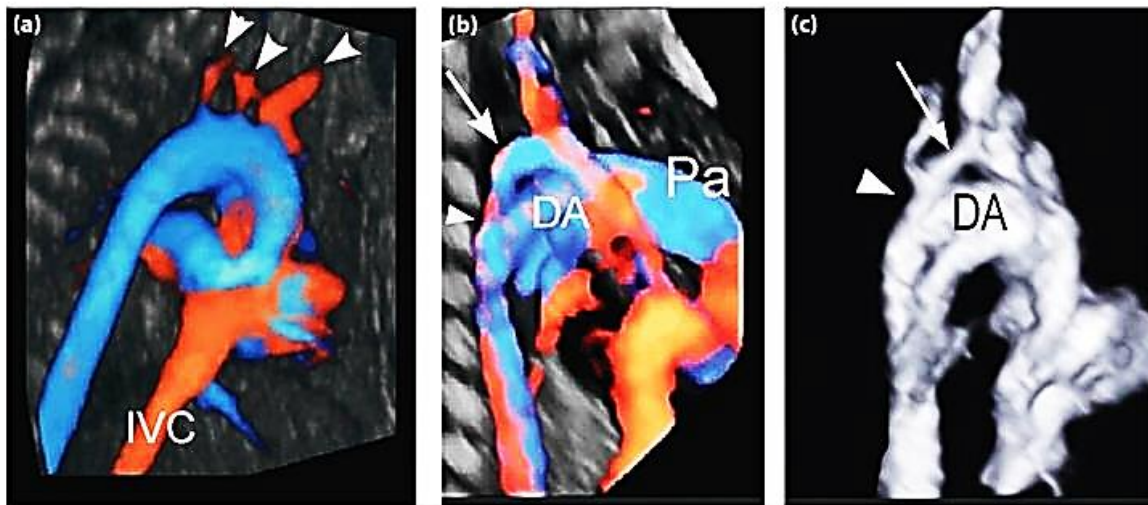
Counseling:

The overall prognosis will depend on several factors, including karyotype, associated extracardiac malformations and cardiac anatomy. Prenatal counseling should therefore take into consideration all the aspects in addition to the well-established fact that the pulmonary outflow obstruction may evolve during pregnancy. With regard to survival, case series of patients with isolated TOF report long term survival rates as high as 80-90%. In conclusion, if no unfavourable prognostic factors are found in utero and, above all, after birth, TOF is an easily correctable heart defect with excellent survival and good quality of life.

Coarctation of Aorta:

Coarctation is discrete narrowing of the aortic arch, most commonly distal to the left subclavian artery. It accounts for 7% of all congenital cardiac defects [11] and 6% of cardiac anomalies seen prenatally [12]. It can be associated with chromosomal abnormalities, maternal diabetes, bicuspid valve, aortic stenosis, Turner syndrome, intracranial aneurysms, VSD, ASD, Shone complex, transposition, Taussig-Bing anomaly, and aortic hypoplasia. Coarctation may be difficult to visualize in ultrasound and is diagnosed when the distal arch is smaller than normalized values. In hypoplasia, the entire arch is small (Fig.). In addition, the ascending aorta

is small (ratio of the PA to the ascending aorta, $>2SD$ above normal). The LV can be small when it is part of the hypoplastic LV syndrome. Coarctation may progress in utero [1].



Coarctation of the aorta. Four-dimensional echocardiography (STIC) contributes to the characterization of aortic coarctation. Volumes should be acquired with a longitudinal ventral approach for adequate imaging. (a) Normal fetus at 22 weeks of gestation. Glassbody rendering shows the normal size of the aortic arch and the three neck vessels (arrowheads). The isthmic tract shows no indentation or reduction in caliber. (b) In a fetus with aortic coarctation (26 weeks of gestation), the same view demonstrates the tapered, hypoplastic aortic arch (arrow) and the much greater size of the ductal arch. The arrowhead indicates the shelf. (c) In another case of severe aortic coarctation, B-flow demonstrates (even more clearly than with glassbody) both the tapering (arrow) and the shelf (arrowhead), which represent classic findings in severe aortic coarctation. DA: ductal arch; IVC: inferior vena cava; Pa: pulmonary artery.



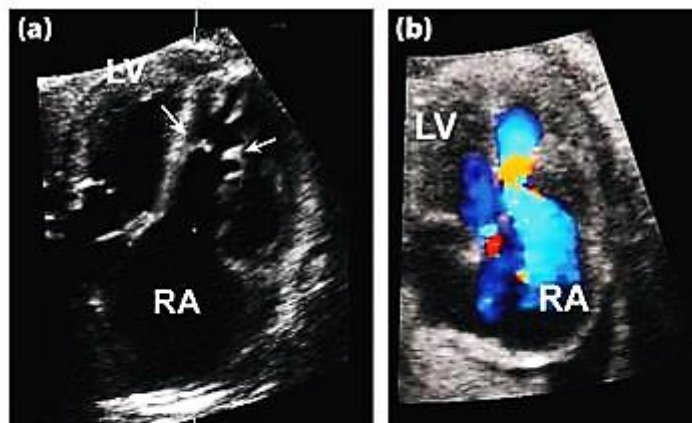
Coarctation of the aorta. (a) On the four-chamber view, the ventricular disproportion, which is an indirect sign of coarctation, is evident (the right ventricle is larger than the left). (b) The three-vessel view demonstrates the severe narrowing of the aorta (A), between the pulmonary artery (P) and the superior vena cava (C). (c) In this case, the coarctation was severe: the extreme discrepancy between the size of the ductal arch (DA) and that of the hypoplastic transverse part of the arch (AO) is evident. (d) In this case of critical coarctation (tubular hypoplasia), on color Doppler, a complete inversion of the flow in the distal part of a hypoplastic aortic arch (AOA) can be seen. AD: ductal arch.

Counseling:

The overall prognosis depends on the severity of the lesion, on the presence of associated cardiac and extracardiac lesions that can significantly influence operative mortality and the life expectancy, and on correct perinatal management. The overall mortality rate is less than 5% for isolated coarctation. In symptomatic neonatal cases with associated cardiac lesions, the mortality rate is about 20%, ranging from 2% in cases associated with VSD to 40% in cases associated with complex cardiac anomalies or when the preoperative clinical condition is poor.

Ebstein's Anomaly:

Ebstein anomaly is characterized by displacement and attachment of one or more tricuspid leaflets (usually septal or posterior leaflets) toward the apex of the RV. The RV is divided into an "atrialized" portion above the leaflets and a muscular portion below the leaflets. It accounts for less than 1% of congenital heart defects, occurs at a rate of 7% in the fetal population, and occurs in 1 per 20,000 live births [1]. It is associated with maternal lithium use, chromosomal abnormalities, ASD, patent foramen ovale, and pulmonary stenosis or atresia. Ultrasound shows apical displacement of the tricuspid valve into the RV, tethered leaflets, reduction in the size of the functional RV (Fig.), increase in the size of the RV (including the atrialized portion), and tricuspid regurgitation. Cardiomegaly, hydrops, and tachyarrhythmias may be seen. Intrauterine mortality is as high as 85%. Differential diagnosis includes Uhl anomaly, tricuspid valve dysplasia, and idiopathic RA enlargement [1]



Ebstein's anomaly (35 weeks of gestation). (a) Image showing the significant displacement of the tricuspid annulus within the right ventricle, with the dysplastic posterior and septal leaflets adhering to the interventricular septum (arrows). The consequent severe insufficiency is responsible for the huge cardiomegaly. (b) Color Doppler demonstrating the severe tricuspid insufficiency, with aliasing and turbulence at the level of the downwardly displaced valve (orange area).

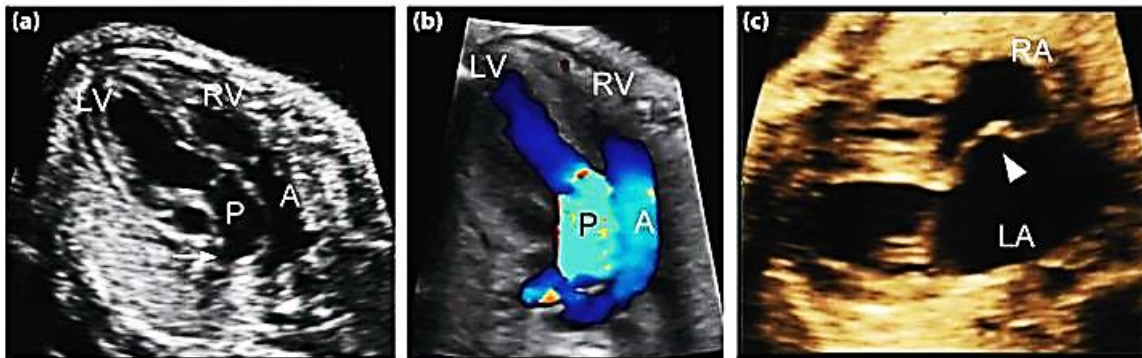
Counseling:

Defining the outcome of Ebstein's anomaly is difficult bearing in mind that there are cases who die in utero and cases who live an almost normal life. As mentioned in this section, most of the cases detected in utero are at the worse end of the spectrum, often showing severe cardiomegaly and heart

failure. This is due to the fact that only those cases in which the four-chamber view is severely abnormal are recognized in utero. In fetal series, the overall intrauterine mortality rate is as high as 40%; 20%-30% die in the neonatal period, and the remaining 30% survive more than one month. Neonates with Ebstein's anomaly requiring intensive care have a 50% mortality rate, but if they survive more than one month, then the life expectancy increases.

Transposition of Great Vessels:

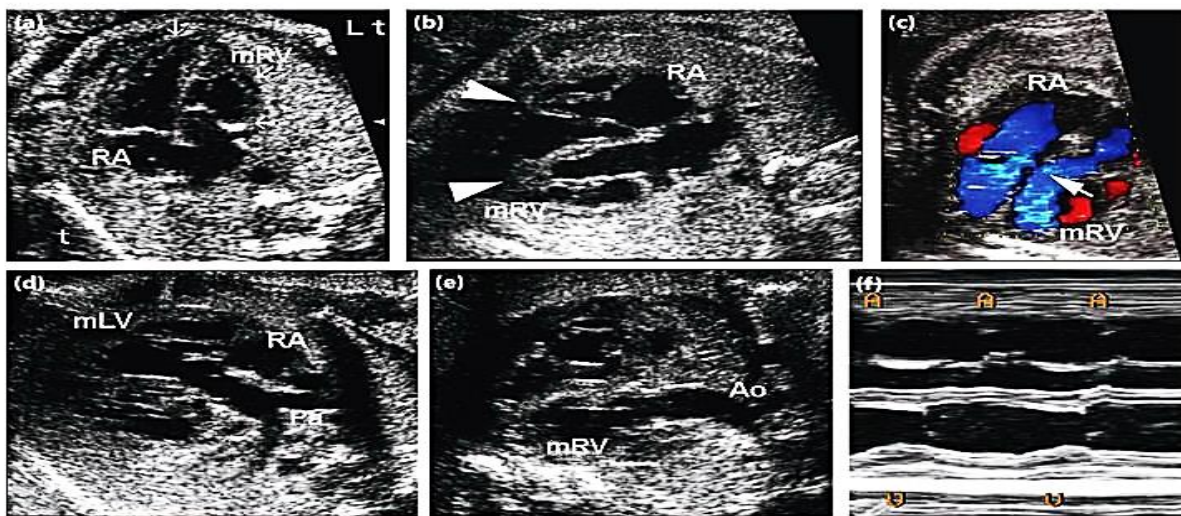
Transposition of great arteries is characterized by the abnormal origin of the great arteries from the ventricles because of abnormal spiraling of the conotruncal septum. It is broadly divided into D and L types. D-trans-position accounts for 80% of transpositions and is characterized by the aorta originating from the morphologic RV and the PA originating from the morphologic LV. The pulmonary and systemic circulations operate in parallel, rather than serial, circuits. Oxygenation of systemic blood requires mixing via ASD, VSD, or patent ductus arteriosus. On ultra-sound, the morphologic RV is located on the right side of the morphologic LV. The artery originating from the morphologic RV (i.e., aorta) gives off branches to the head and neck, whereas the artery originating from the morphologic LV (i.e., PA) bifurcates and there is a sharp angle of the left PA with the ductus, giving the classic "baby bird beak" sign. The aorta and PA do not cross but are parallel to each other (Fig.), with the aorta anterior and to the right of the PA [5]. In congenitally corrected transposition (L-transposition), in addition to the ventriculoarterial concordance, there is also AV discordance with the morphologic LA connected to the morphologic RV and the morphologic RA connected to the morphologic LV. L-transposition accounts for 1% of congenital heart defects and may be associated with VSD and pulmonic stenosis. Ultrasound shows parallel aorta and PA with the aorta anterior and to the left of the PA. The tricuspid valve may be deformed and inferiorly displaced. Differentiating this from D-trans-position of great arteries requires identification of the morphologic RV and LV.



Transposition of the great arteries (TGA), 27 weeks of gestation. (a) On the left outflow tract view, the ventriculoarterial discordance and the absence of crossover (two parallel vessels) are demonstrated, with the pulmonary artery arising from the left ventricle and the anterior aorta arising from the right ventricle. (b) Color Doppler helps in defining the ventriculoarterial connection and the parallel course of the vessels. (c) In the case of TGA with an intact ventricular septum, a restrictive foramen ovale (arrowhead) indicates the need for immediate postpartum Rashkind atrioseptostomy (see this chapter's text).

Counseling:

TGA represents a keystone in the validation of prenatal screening of CHD, as it represents the ideal model of CHD to be screened: it has a high early neonatal mortality risk, which disappears if early neonatal management is properly planned; and, once corrected, this CHD has a greater than 90% long-term survival rate in good functional conditions. Once corrected, patients with TGA experience a 15-year survival rate of 86%.



Corrected transposition of the great arteries (cTGA), 31 weeks of gestation. (a) On the four-chamber view, the morphologic right ventricle (mRV) is connected with the left atrium, and, vice versa, the morphologic left ventricle is connected with the right atrium. Note the moderator band in the mRV and the Ebstein-like appearance of the left-sided tricuspid valve. (b) On the transverse four-chamber view, the differential insertion of the papillary muscles is evident: the tricuspid ones attach to the apex of the ventricle, whereas the mitral one attaches to the lateral free ventricular wall. (c) Color Doppler is used to demonstrate a small VSD not visible on grayscale ultrasound (arrow). (d) The right outflow tract view demonstrates the pulmonary artery (with the bifurcation) arising from the right-sided left ventricle. (e) The left outflow tract view demonstrates the aorta arising from the left-sided mRV. (f) A complete heart block can sometimes appear in the third trimester. Note the dissociation between the atrial (A) and ventricular (V) frequencies.

Counseling:

The overall prognosis of cTGA is one of the most controversial and debated issues in pediatric cardiology. The frequency and severity of the associated cardiac lesions represent the most important determinants of

survival and mortality. In particular, severe insufficiency of the left-sided tricuspid valve and impaired systolic function of the right (systemic) ventricle are the main indicators of a poor prognosis.

MRI:

The role of fetal MRI as a complementary tool to ultrasound in fetal imaging has grown exponentially since the first reports in 1985 [23, 24]. Unlike ultrasound imaging, this modality is not affected by maternal and fetal conditions such as obesity and oligohydramnios [25], which particularly impair sonographic visualization of the fetal heart; maternal obesity increases the rate of sub-optimal ultrasound visualization of the fetal cardiac structures by 49.8% [26], despite advanced ultrasound equipment. Recent studies have described the potential role of fetal MRI in the evaluation of the anatomy and pathology of the cardiovascular system [27, 28]; however, most studies as of yet had only healthy fetuses in their study population. The most efficient technique to characterize the fetal cardiac anatomy, according to the literature, appears to be T2-weighted true fast imaging with steady-state precession sequence, whereas the most suitable technique to evaluate the fetal cardiac function is with real-time cine-MRI.

Conclusion

Routine fetal cardiac ultrasound using four-chamber and outflow-tract views enables the detection and characterization of most of the cardiac anomalies. A further comprehensive evaluation can be performed with fetal echocardiography, particularly in high-risk pregnancies and extracardiac anomalies. Doppler imaging is used in the evaluation of vascular and valvular lesions. Three-dimensional imaging enables reconstruction of multiple complex planes from a single transverse acquisition. Four-dimensional imaging enables cine looping of images in multiple planes, enabling estimation of cardiac motion and function. MRI is a complementary tool, especially when fetal cardiac structures are visualized suboptimally with ultrasound.

References:

1. Stamm ER, Drose JA. The fetal heart. In: Rumack CA, Wilson SR, Charboneau WJ, eds. *Diagnostic ultrasound*, 2nd ed. St. Louis, MO: Mosby, 1998: 1123–1159

2. Small M, Copel JA. Indications for fetal echocardiography. *PediatrCardiol*2004;25:210–222
3. Carvalho JS, Ho SY, Shinebourne EA. Sequential segmental analysis in complex fetal cardiac abnormalities: a logical approach to diagnosis. *Ultrasound Obstet Gynecol*2005;26:105–111
4. International Society of Ultrasound in Obstetrics and Gynecology. Cardiac screening examination of the fetus: guidelines for performing the “basic” and “extended basic” cardiac scan. *Ultrasound Obstet Gynecol*2006;27:107–113
5. Naderi S, McGahan JP. A primer for fetal cardiac imaging: a stepwise approach for 2-D imaging. *Ultrasound Q*2008;24:195–206
6. Allan L. Technique of fetal echocardiography. *PediatrCardiol*2004;25:223–233
7. Sklanksy M. Advances in fetal cardiac imaging. *PediatrCardiol*2004;25:307–321
8. Barboza JM, Dajani NK, Glenn LG, et al. Prenatal diagnosis of congenital cardiac anomalies: a practical approach using two basic views. *Radio-Graphics*2002;22:1125–1138
9. Collett RW, Edwards JE. Persistent truncus arteriosus: a classification according to anatomic types. *Surg Clin North Am*1949;29:1245–1270
10. Hawkins JA, Dody DB. Aortic atresia: morphologic characteristics affecting survival and operative palliation. *J Thorac Cardiovasc Surg*1984;88:620–626
11. Kimura-Hayama ET, Melendez G, Mendizabal AL, et al. Uncommon congenital and acquired aortic diseases: role of multidetector CT angiography. *RadioGraphics*2010;30:79–98
12. Allan LD, Crawford DC, Anderson RH, et al. The spectrum of congenital heart disease detected echocardiographically in prenatal life. *Br Heart J*1985;54:523–526
13. Ho ML, Bhalla S, Bierhals A, Gutierrez F. MDCT of partial anomalous pulmonary venous return in adults. *J Thorac Imaging*2009;24:89–95
14. Gao Z, Duan QJ, Zhang ZW, Ying LY, Ma LL. Pentalogy of Cantrell associated with thoracoabdominal ectopia cordis. *Circulation*2009;119:e483–e485
15. Isaacs H. Fetal and neonatal cardiac tumors. *PediatrCardiol*2004;25:252–273
16. Lacey SR, Donofrio MT. Fetal cardiac tumors: prenatal diagnosis and

- outcome. *PediatrCardiol*2007;28:61–67
17. Pedra SRFF, Smallhorn JF, Ryan G, et al. Fetalcardiomyopathies:pathogenicmechanisms,hemodynamicfindings,an dclinicaloutcome.*Circulation*2002;106:585–591
 18. YinonY, YagelS, HegeshJ,etal.Fetalcardiomyopathy: in utero evaluation and clinical significance.*PrenatDiagn*2007;27:23–28
 19. TrastourC, BafghiA, DelotteJ,etal.Earlyprenatal diagnosis of endocardial fibroelastosis. *UltrasoundObstetGynecol*2005; 26:303–306
 20. Bromley B, Lieberman E, Shipp TD, RichardsonM, Benacerraf BR. Significance of an echogenicintracardiacfocusinfetusesathighandlowriskforaneuploidy.*JUltrasoundMed*1998;17:127–131
 21. Nyberg DA, Souter VL, El-Bastawissi A, YoungS,LuthhardtF,LuthyDA.Isolatedsonographic markers for detection of fetal Down syndrome inthe second trimester of pregnancy. *J UltrasoundMed*2001;20:1053–1063
 22. Kleinman CS, Nehgme RA. Cardiac arrhythmiasinthehumanfetus.*PediatrCardiol*2004;23:234–251
 23. McCarthy SM, Filly RA, Stark DD, Callen PW, Golbus MS, Hricak H. Magnetic resonance imaging of fetal anomalies in utero: early experience.*AJR*1985;145:677–682
 24. Mazouni C, Gorincour G, Juhan V, Bretelle F.Placenta accreta: a review of current advances inprenataldiagnosis.*Placenta*2007;28:599–603
 25. BenacerrafBR.Examinationofthesecond-trimester fetus with severe oligohydramnios usingtransvaginal scanning. *ObstetGynecol*1990; 75:491–493
 26. Hendler I, Blackwell SC, Bujold E, et al. The impact of maternal obesity on mid trimester sonographic visualization of fetal cardiac and cranio-spinal structures. *Int J ObesRelatMetabDisord*2004;28:1607–1611
 27. Gorincour G, Bourlière-Najean B, Bonello B, etal. Feasibility of fetal cardiac magnetic resonanceimaging:preliminaryexperience.*UltrasoundObstetGynecol*2007;29:105–110
 28. Chung T. Assessment of cardiovascular anatomyin patients with congenital heart disease by magnetic resonance imaging. *PediatrCardiol*2000;21:18–26.